



西安交通大学
XI'AN JIAOTONG UNIVERSITY



中国科学院高能物理研究所
Institute of High Energy Physics
Chinese Academy of Sciences

Simulation of Irradiation Damage and Defect Evolution Induced by Neutrons in LGAD

DRD3 Week, CERN, Dec. 2024

Presenter: LI, Wei

E-mail:

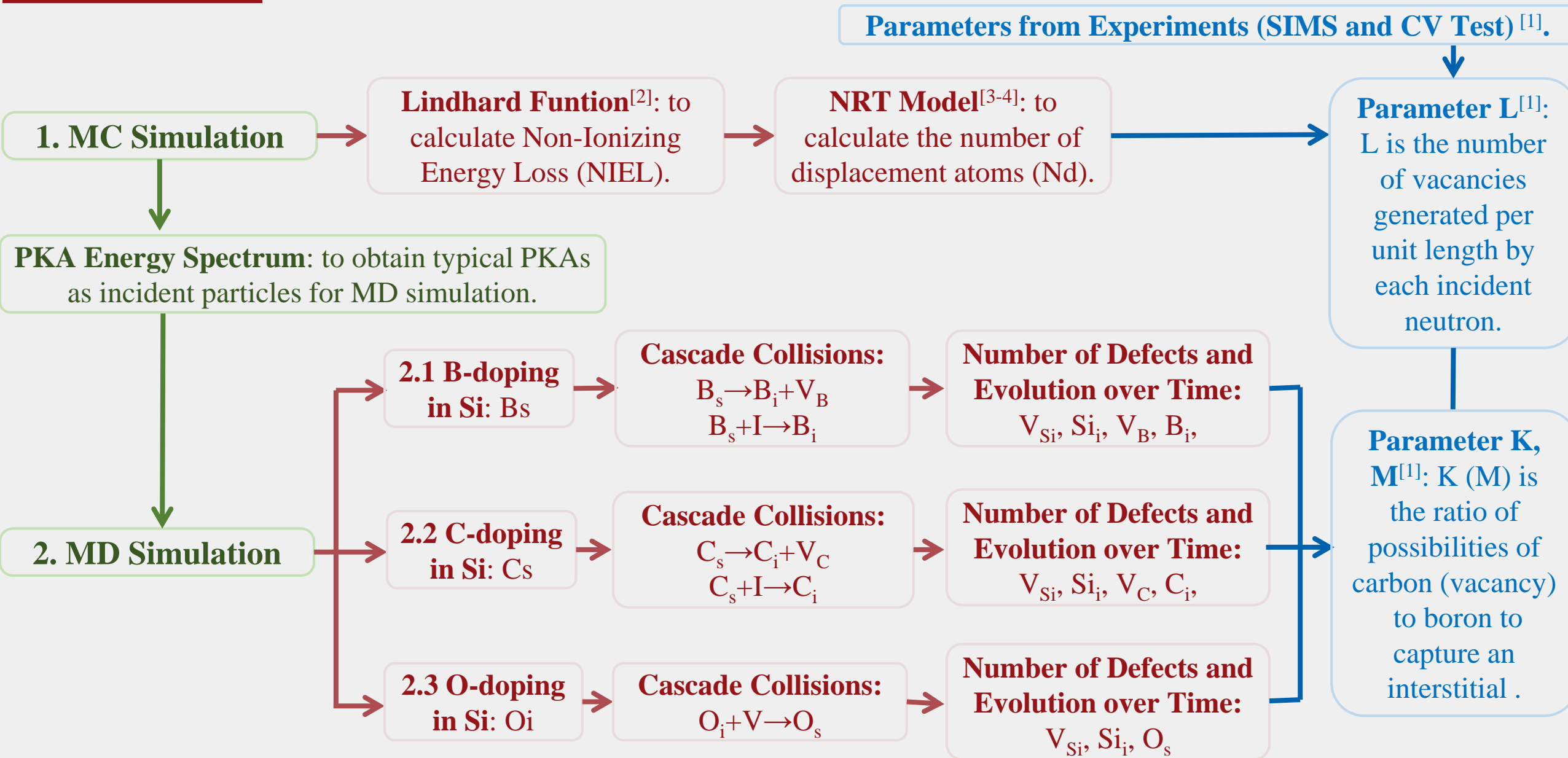
nuclear@stu.xjtu.edu.cn (Presenter)

fanyy@ihep.ac.cn (Corresponding Author)

Motivation

- Low Gain Avalanche Detectors(LGAD) with carbon implantation by IHEP have excellent **irradiation resistance**.
- Its irradiation resistance originates from **the protective effect of doped carbon on the acceptor boron**.
- To provide an **atomic-level explanation of how carbon-doping mitigates acceptor removal**.

Outline

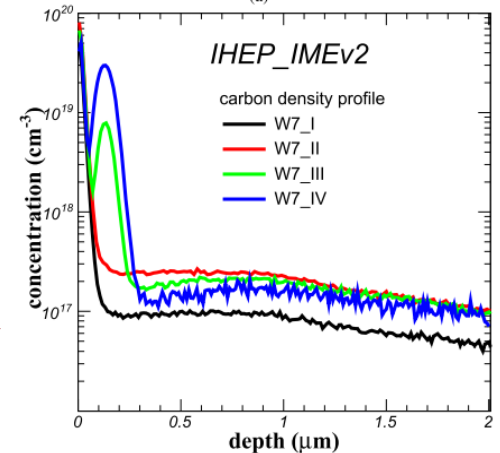


Three assumptions to be considered in simulation:

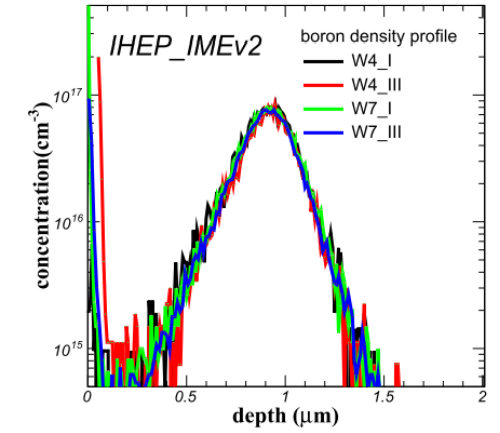
- **Actual doping concentration (data obtained through SIMS^[1]):**
B-doping: $1E17 \text{ cm}^{-3}$; C-doping: $2E17 \text{ cm}^{-3}$; O-doping: $2E17 \text{ cm}^{-3}$;
- **Doping concentration in this MD simulation:**
B/C/O-doping: $2.8E22 \text{ cm}^{-3}$ (One dopant atom per $2 \times 2 \times 2$ silicon supercell (64 atoms)).

- **Actual dimensions of the supercell that should be simulated in MD:**
 $150 \times 150 \times 150$ supercell, i.e., $814.7 \times 814.7 \times 814.7 \text{ \AA}^3$ (Considering the projectile range of PKA);
- **Dimensions in this MD simulation:**
 $50 \times 50 \times 50$ supercell, i.e., $271.99 \times 271.99 \times 271.99 \text{ \AA}^3$; $1E6$ atoms.

- **Actual initial existence form of B/C/O doping in Si lattice:**
B-doping: B_s (Substitution); C-doping: $C_s + C_i$; O-doping: O_i ;
- **Initial existence form of B/C/O doping in this MD simulation:**
B: B_s ; C: C_s ; O: O_i



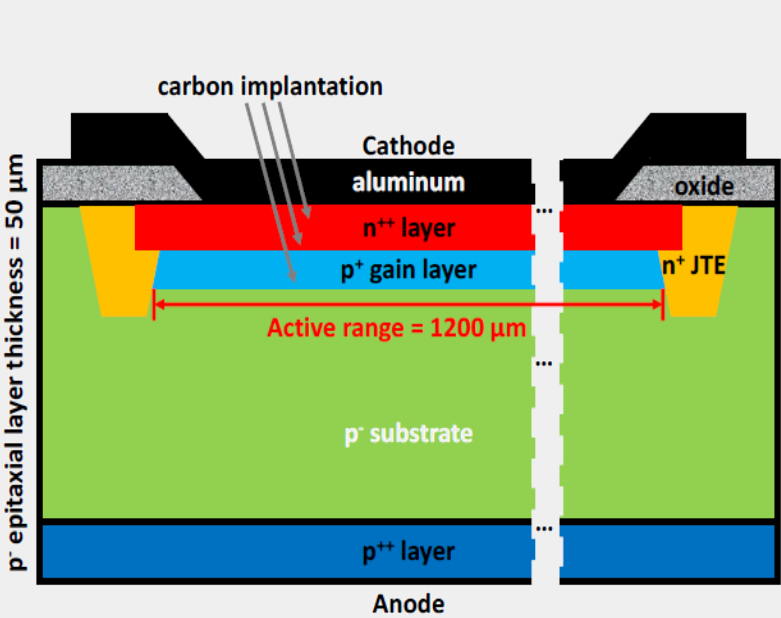
Carbon Density Profile^[1]



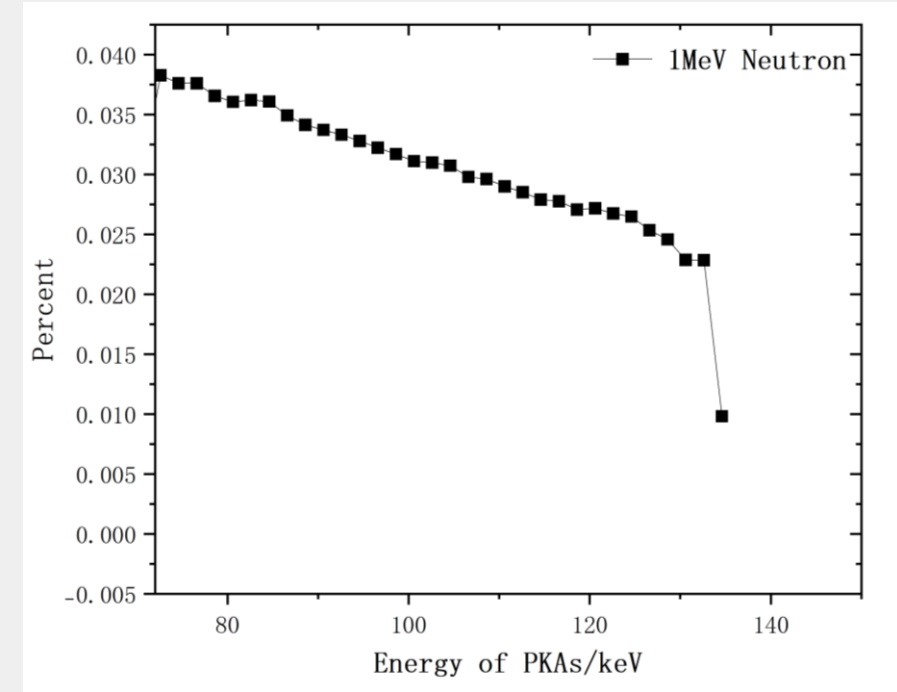
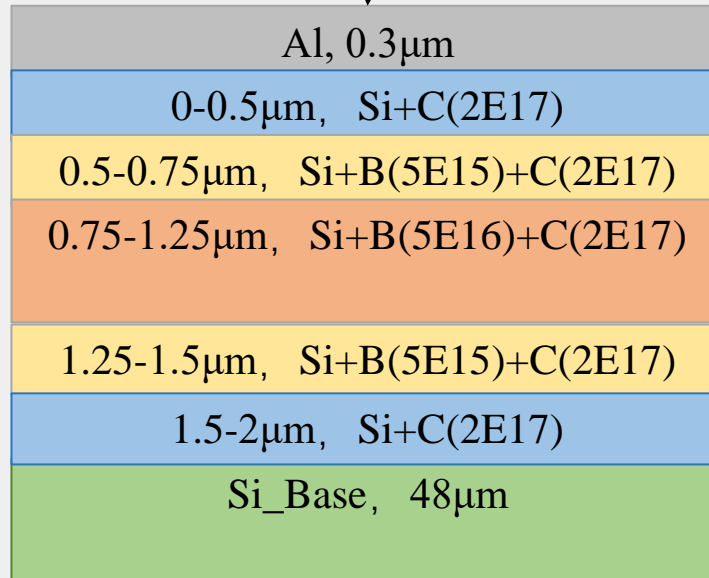
Boron Density Profile^[1]

1

Monte Carlo (MC) Simulations



1MeV neutron



PKA Energy Spectrum (1MeV Neutron)

Thus, **72.6 keV Si-PKA** will be used as the input parameter for MD simulation.

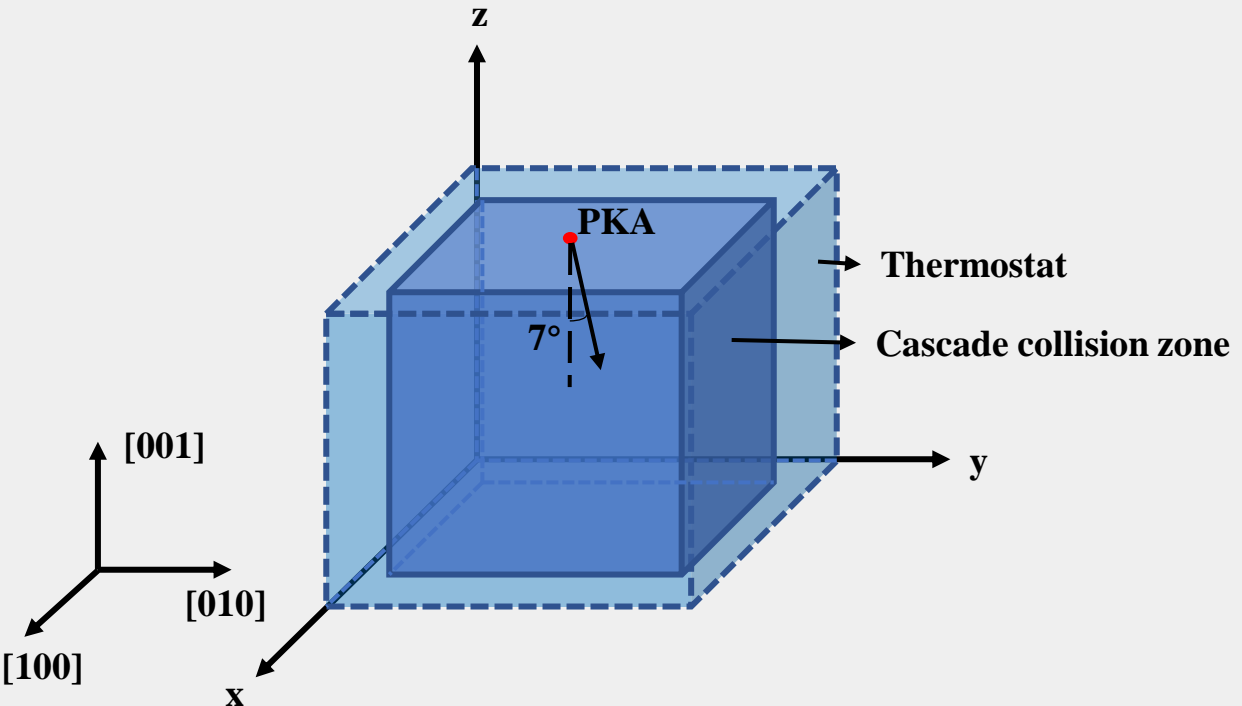
- **Physics List:** QGSP_BIC; G4ScreenedNuclearRecoil^[5-6]
- **Particle Source:** Point Source (1MeV Neutron); Perpendicular Incidence; 1E9
- **Theoretical Model:** Lindhard Funtion; Norgett-Robinson-Torrens (NRT) Model

Average Nd per neutron	L in Experiments /cm ⁻¹	L in Simulation /cm ⁻¹	Discrepancy of L / %
0.295234899	52.5	59.047	12.5

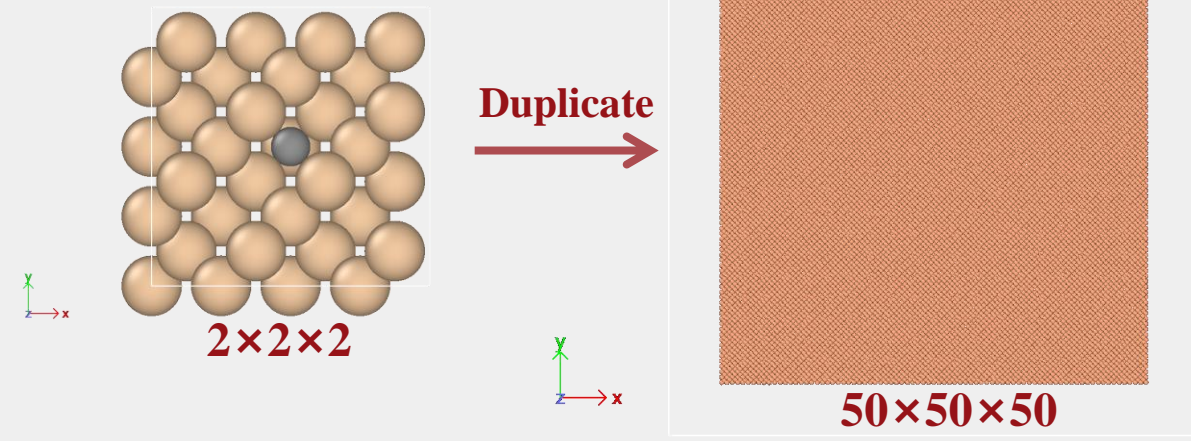
$$L = \frac{\text{Average Nd per neutron}}{h} = \frac{0.2952}{50\mu\text{m}} = 59.047 \text{ cm}^{-1}$$

2

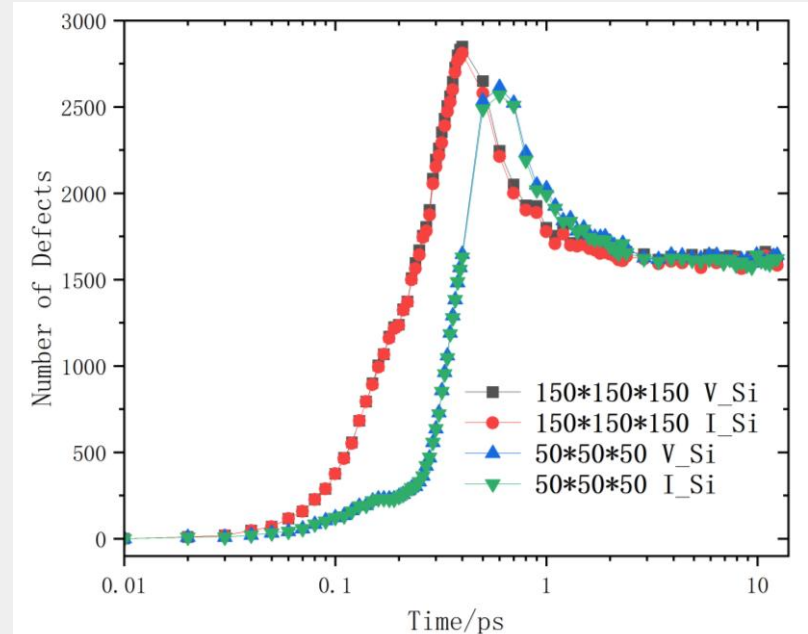
Molecular Dynamics (MD) Simulations



MD Modeling of Cascade Collision Systems in Silicon



- **Supercell:** $50 \times 50 \times 50$, i.e., $271.99 \times 271.99 \times 271.99 \text{ \AA}^3$
- **Doping Concentration:** One dopant atom per $2 \times 2 \times 2$ silicon supercell (64 atoms).



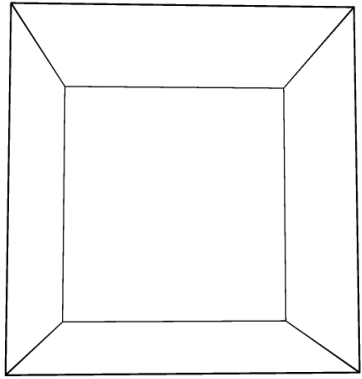
Defect Evolution Over Time (Different Supercells)

Thus, We proved that a $50 \times 50 \times 50$ supercell can be used to replace a $150 \times 150 \times 150$ supercell.

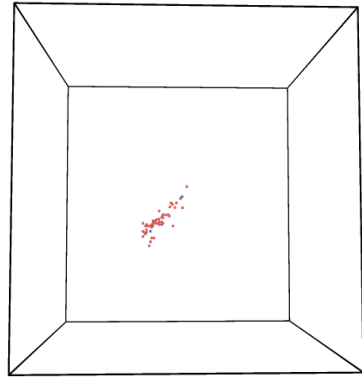
2

Molecular Dynamics (MD) Simulations

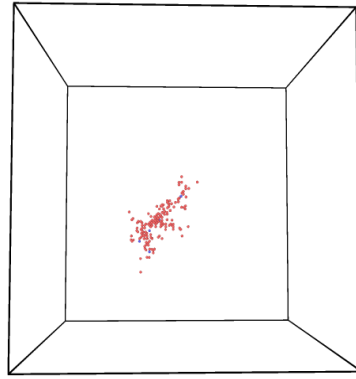
(1) B-Doping in Si (Interatomic Potential : Stillinger-Weber (SW) [7-10])



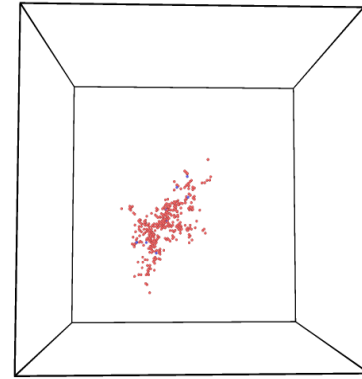
0ps



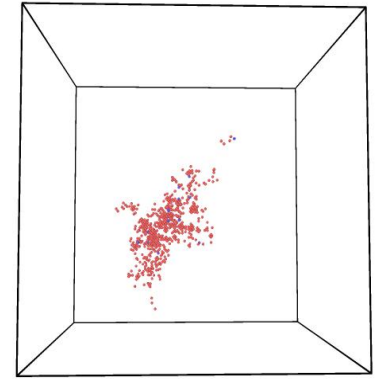
0.02ps



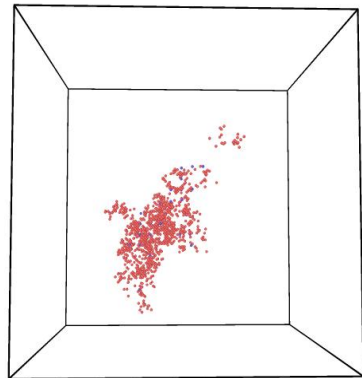
0.04ps



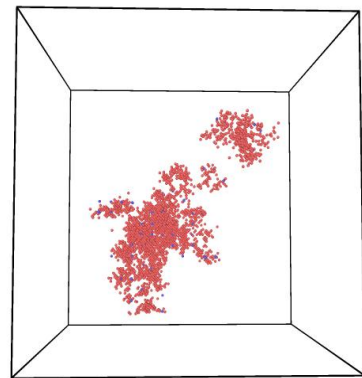
0.06ps



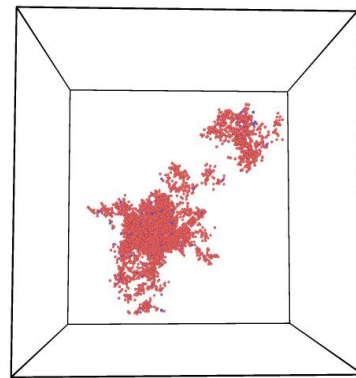
0.08ps



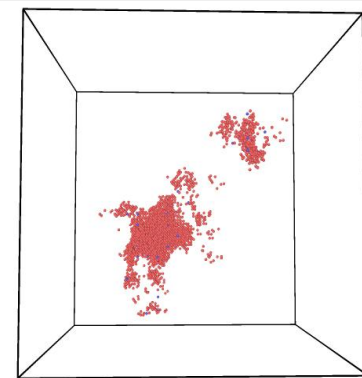
0.1ps



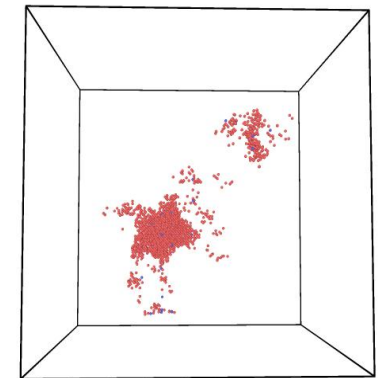
0.2ps



0.4ps

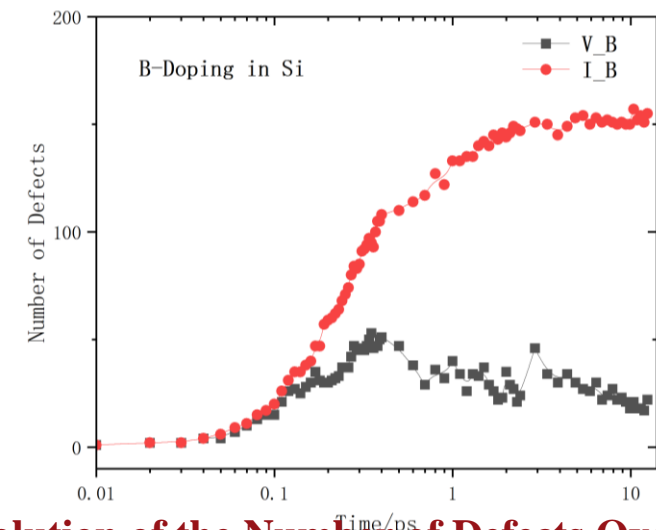
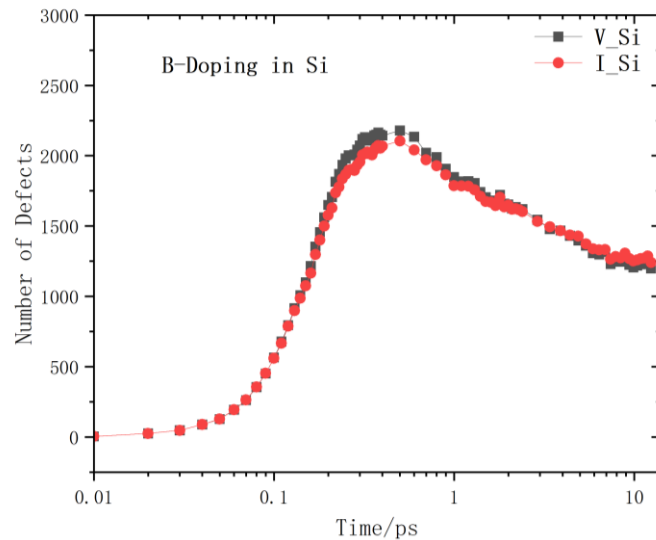


2.4ps



12.4ps

(1) B-Doping in Si (Interatomic Potential : Stillinger-Weber (SW))



Parameter K is the ratio of possibilities of carbon to boron to capture an interstitial, which is 0.65.

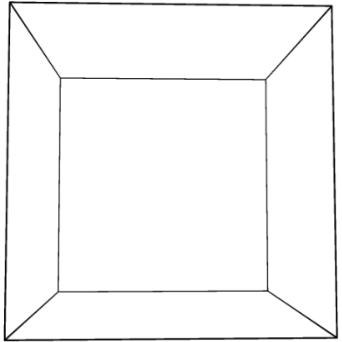
$$K = 2 * \frac{C_i - V_C}{B_i - V_B} = 2 * \frac{C_i - V_C}{159}$$

- **Actual doping concentration (data obtained through SIMS^[1]):**
B-doping: 1E17 cm⁻³; C-doping: 2E17 cm⁻³; O-doping: 2E17 cm⁻³;
- **Doping concentration in this MD simulation:**
B/C/O-doping: 2.8E22 cm⁻³ (One dopant atom per 2×2×2 silicon supercell (64 atoms)).

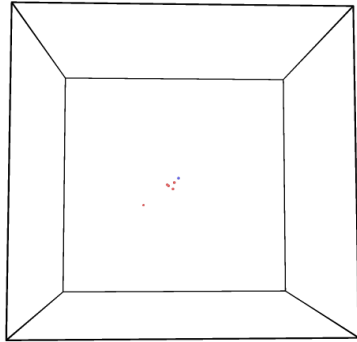
2

Molecular Dynamics (MD) Simulations

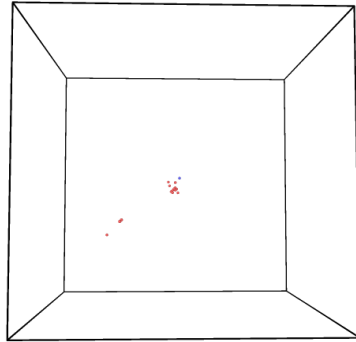
(2) C-Doping in Si (Interatomic Potential : Tersoff/ZBL [11-12])



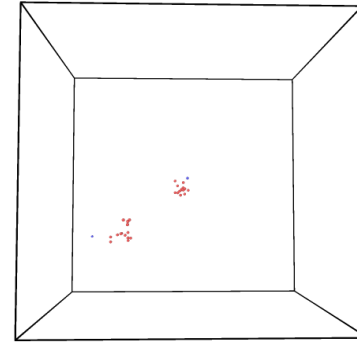
0ps



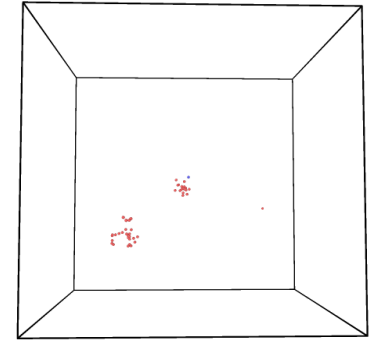
0.02ps



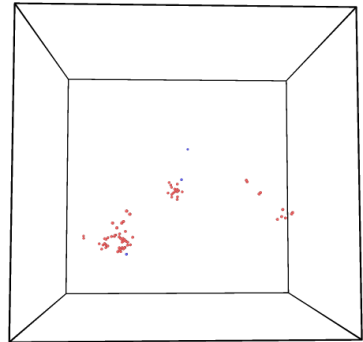
0.04ps



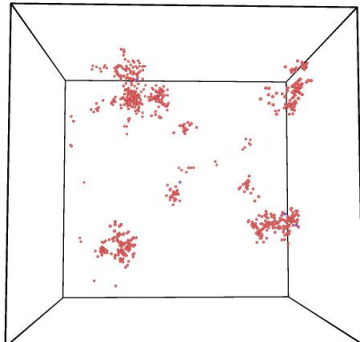
0.06ps



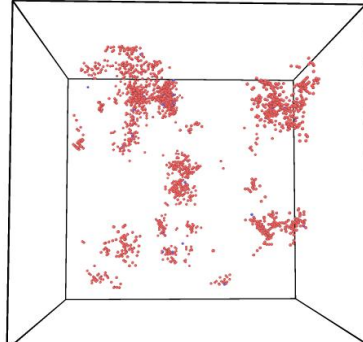
0.08ps



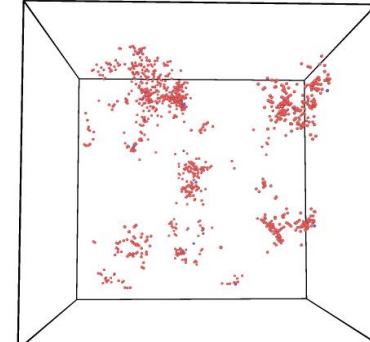
0.1ps



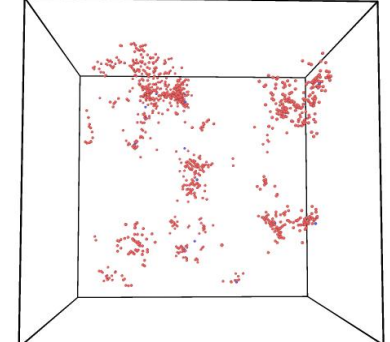
0.2ps



0.4ps



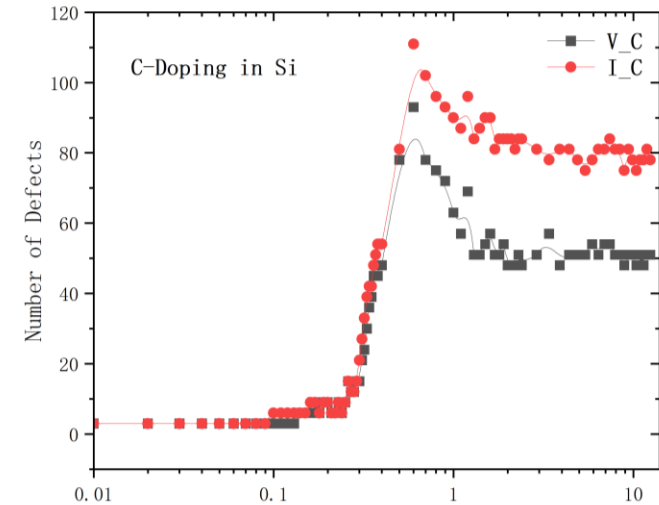
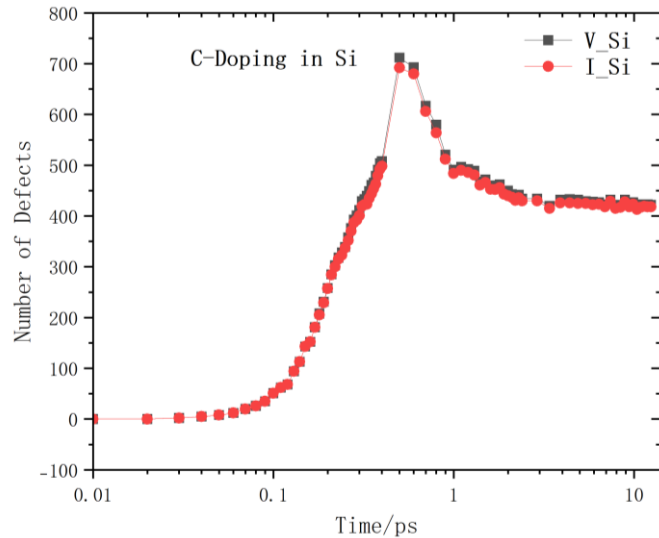
2.4ps



12.4ps

Spatial Distribution of All Vacancies and Interstitial Defects (C-Doping in Si)

(2) C-Doping in Si (Interatomic Potential : Tersoff/ZBL)



Parameter **K** is the ratio of possibilities of carbon to boron to capture an interstitial, which is 0.65.

$$K = 2 * \frac{C_i - V_C}{B_i - V_B} = 2 * \frac{C_i - V_C}{159} = 2 * \frac{27}{159} = 0.34$$

Parameters	From Experiments ^[1]	From this simulation	Discrepancy / %
L	52.5 /cm	59.047 /cm	12.5
K	0.65	0.34	47.7
M	9.5	—	—

- Actual initial existence form of B/C/O doping in Si lattice: B-doping: B_s (Substitution); C-doping: C_s+C_i; O-doping: O_i;
- Initial existence form of B/C/O doping in this MD simulation: B: B_s; C:C_s; O:O_i

3 Summary & Outlook

Completed:

- We have calculated $L_{\text{simulation}} = 59.047$ /cm through MC simulations, which corresponds to 59.047 vacancies generated per unit length per incident neutron. $L_{\text{simulation}} = 59.047$ /cm shows a very high degree of consistency with $L_{\text{experiment}} = 52.5$ /cm.
- We have also calculated $K_{\text{simulation}} = 0.34$ through MD simulations, meaning the ratio of probabilities for carbon to boron to capture an interstitial is 0.34, while $K_{\text{experiment}} = 0.65$. The discrepancy may arise because the types of carbon defects capable of capturing interstitials are not limited to substitutional carbon defects.
- We explained how doped carbon protects the acceptor boron with parameter L, K and M: carbon competes to capture silicon defects, thereby "clearing" or "reducing" the silicon defects around the boron acceptor, thereby protecting the acceptor boron. That is to say, carbon indirectly protects boron by reducing silicon defects, rather than directly acting on boron.

To be completed:

- In **MD simulation work**, the types and numbers of irradiation-induced defects in O-doping conditions are being calculated. For C-doping, possibilities of Ci to capture defects needs to be considered.
- **KMC simulation work** has been initiated. Based on the results of MD simulations, the defect numbers and spatial distributions obtained from MD are used as input parameters for KMC simulation. This enables the study of larger systems and longer time scales to determine the probabilities of different doping atoms to capture defects.

**Thank you for your
attention!**

Formula mentioned

1) MC Section

- **Lindhard Funtion** [2]: to calculate NIEL.

$$Q(T) = \frac{1}{1 + k_L g(\varepsilon)}$$

$$\varepsilon = \frac{T}{30.724 Z Z_L \left(Z^{\frac{2}{3}} + Z_L^{\frac{2}{3}} \right)^{\frac{1}{2}} \left(1 + \frac{A}{A_L} \right)}$$

$$k_L = \frac{0.794 Z^{\frac{2}{3}} Z_L^{\frac{1}{2}} (A + A_L)^{\frac{3}{2}}}{\left(Z^{\frac{2}{3}} + Z_L^{\frac{2}{3}} \right)^{\frac{3}{4}} A^{\frac{3}{2}} A_L^{\frac{1}{2}}}$$

$$g(\varepsilon) = \varepsilon + 0.40244 \varepsilon^{\frac{3}{4}} + 3.4008 \varepsilon^{\frac{1}{6}}$$

- **QGSP_BIC physical model simulation** includes electromagnetic interactions (multiple scattering, ionization, photoelectric effect, and bremsstrahlung) and hadronic interactions (elastic scattering, inelastic scattering, and nuclear reactions).
- **G4_ScreenedNuclearRecoil** class has been added to electromagnetic interactions to simulate the nuclear stopping power of recoiling atoms. This class, developed by Weller et al. [13], is suitable for calculating the Non-Ionizing Energy Loss (NIEL) produced by proton and neutron incidence on materials such as Si and GaAs. [14]
- **NRT Model** [3-4]: to calculate the number of displacement atoms. For Si, $E_d = 28 \text{ eV}$.

$$N_d(T) = \begin{cases} 0 & T > E_d \\ 1 & E_d \leq T \leq 2.5 E_d \\ \frac{0.8(T)}{2 E_d} & T \geq 2.5 E_d \end{cases}$$

Formula mentioned

2) MD Section

- Interatomic Potential Function: Stillinger-Weber (SW) for Si-B [7-10]

$$E = \sum_i \sum_{j>i} \phi_2(r_{ij}) + \sum_i \sum_{j \neq i} \sum_{k>j} \phi_3(r_{ij}, r_{ik}, \theta_{ijk})$$

$$\phi_2(r_{ij}) = A_{ij} \epsilon_{ij} \left[B_{ij} \left(\frac{\sigma_{ij}}{r_{ij}} \right)^{p_{ij}} - \left(\frac{\sigma_{ij}}{r_{ij}} \right)^{q_{ij}} \right] \exp \left(\frac{\sigma_{ij}}{r_{ij} - a_{ij} \sigma_{ij}} \right)$$

$$\phi_3(r_{ij}, r_{ik}, \theta_{ijk}) = \lambda_{ijk} \epsilon_{ijk} [\cos \theta_{ijk} - \cos \theta_{0ijk}]^2 \exp \left(\frac{\gamma_{ij} \sigma_{ij}}{r_{ij} - a_{ij} \sigma_{ij}} \right) \exp \left(\frac{\gamma_{ik} \sigma_{ik}}{r_{ik} - a_{ik} \sigma_{ik}} \right)$$

TABLE VI. Stillinger-Weber parameters for Si-Si and Si-B interactions. Parameters refer to Eqs. (4) and (5) shown in the text. The preferred Si-B-Si bond angle is 114.9°, and the neighbor cutoff is 3.3 Å.

Parameter	Pure silicon potential	Si-B potential
A	15.2764 eV	24.2407 eV
B	0.602 224	0.708 769
p	4.0	5.996 808
q	0.0	4.292 801
a	1.8	1.861 019
λ	45.5070 eV	40.8000 eV
γ	1.2	1.866 938
κ	$\frac{1}{3}$	0.421 2354
σ	2.09510 Å	2.38 703 Å

- Interatomic Potential Function: Tersoff/ZBL for Si-C [11-12]

$$E = \frac{1}{2} \sum_i \sum_{j \neq i} V_{ij}$$

$$V_{ij} = (1 - f_F(r_{ij} + \delta)) V^{ZBL}(r_{ij} + \delta) + f_F(r_{ij} + \delta) V^{Tersoff}(r_{ij} + \delta)$$

$$f_F(r) = \frac{1}{1 + e^{-A_F(r-rc)}}$$

$$V^{ZBL}(r) = \frac{1}{4\pi\epsilon_0} \frac{Z_1 Z_2 e^2}{r} \phi(r/a)$$

$$a = \frac{0.8854 a_0}{Z_1^{0.23} + Z_2^{0.23}}$$

$$\phi(x) = 0.1818e^{-3.2x} + 0.5099e^{-0.9423x} + 0.2802e^{-0.4029x} + 0.02817e^{-0.2016x}$$

$$V^{Tersoff}(r) = f_C(r) [f_R(r) + b_{ij} f_A(r)]$$

$$f_C(r) = \begin{cases} 1 & r < R - D \\ \frac{1}{2} - \frac{1}{2} \sin \left(\frac{\pi}{2} \frac{r-R}{D} \right) & R - D < r < R + D \\ 0 & r > R + D \end{cases}$$

$$f_R(r) = A \exp(-\lambda_1 r)$$

$$f_A(r) = -B \exp(-\lambda_2 r)$$

$$b_{ij} = (1 + \beta^n \zeta_{ij}^n)^{-\frac{1}{2n}}$$

$$\zeta_{ij} = \sum_{k \neq i, j} f_C(r_{ik} + \delta) g(\theta_{ijk}) \exp[\lambda_3^m (r_{ij} - r_{ik})^m]$$

$$g(\theta) = \gamma_{ijk} \left(1 + \frac{c^2}{d^2} - \frac{c^2}{[d^2 + (\cos \theta - \cos \theta_0)^2]} \right)$$

Reference

- [1] [Y. Feng et al. IEEE Transactions on Nuclear Science 69.12 \(2022\): 2324-2329.](#)
- [2] [Torrens, I. M., et al. Interatomic Potentials and Simulation of Lattice Defects. Boston, MA: Springer US, 1972. 423-436.](#)
- [3] [Norgett, M. J., et al. Nuclear engineering and design 33.1 \(1975\): 50-54.](#)
- [4] [Inguibert, C., et al. 2009 European Conference on Radiation and Its Effects on Components and Systems. IEEE, 2009.](#)
- [5] [Walters, R. J., et al. Journal of applied physics 82.5 \(1997\): 2164-2175.](#)
- [6] [Raine, Mélanie, et al. IEEE Transactions on Nuclear Science 64.1 \(2016\): 133-140.](#)
- [7] [Stillinger and Weber, Phys Rev B, 31, 5262 \(1985\).](#)
- [8] [J.-W. Jiang, Nanotechnology 26, 315706 \(2015\).](#)
- [9] [J.-W. Jiang, Acta Mech. Solida. Sin 32, 17 \(2019\).](#)
- [10] [Paul B. Rasband et al, J. Appl. Phys. 79 \(12\), \(1996\).](#)
- [11] [J. Tersoff, Phys Rev B, 37, 6991 \(1988\).](#)
- [12] J.F. Ziegler, J.P. Biersack, U. Littmark, 'Stopping and Ranges of Ions in Matter' Vol1, 1985, Pergamon Press.
- [13] [Walters, R. J., et al. Journal of applied physics 82.5 \(1997\): 2164-2175.](#)
- [14] [Raine, Mélanie, et al. IEEE Transactions on Nuclear Science 64.1 \(2016\): 133-140.](#)